Investigating the DC Performance of Ni/Au and Pt/Au Schottky Gate Contacts on GaN HEMTs for Ku-band Applications

Chanchal[1,2], Khushwant Sehra[1,3]*, Amit Malik[2], Robert Laishram[2], D. S. Rawal[1], and Manoj Saxena[4]

[1]*Department of Electronic Science, University of Delhi, Delhi, India*
[2]*Solid State Physics Laboratory, Defence Research & Development Organization, Delhi, India*
[3]*Department of Electronics and Communication Engineering, Faculty of Technology, University of Delhi, Delhi, India*
[4]*Department of Electronics, Deen Dayal Upadhyaya College, University of Delhi, Delhi, India*

Volume 1, Issue 4, July 2024
Received:13 March, 2024; Accepted: 27 June, 2024
DOI: https://doi.org/10.63015/10S-2421.1.4

**Corresponding Author Email: khushwantsehra@fot.du.ac.in*

Abstract: This manuscript investigates the DC performance of Ni/Au and Pt/Au Schottky Gate contacts on 150 nm AlGaN/GaN HEMTs for Ku band applications. Comparison in terms of the short channel effects (SCEs), in particularly the drain-induced barrier lowering (DIBL), demonstrate the long-term stability of Ni/Au Schottky contacts for mm-wave applications. To assess the reliability of the Schottky metal scheme, the fabricated devices were subjected to a high gate reverse bias step stress of – 30 V with a step of – 5 V. A higher degree of ON–state resistance (R_{ON}) degradation for the Pt/Au Schottky contact evinces remarkable performance of Ni/Au Schottky contacts for mm-Wave applications.

Keywords: AlGaN/GaN HEMT, Barrier Height, Inhomogeneities, Threshold Voltage Shift, OFF – State Stress, Reliability

1. Introduction: The unique intrinsic properties of III – Nitrides, in particularly, the GaN have captured the semiconductor market for future mm – Wave applications [1]. The ability to exhibit high carrier mobilities along with high saturation velocities, make GaN based devices suitable for mm – Wave applications [2]. The apparent high performance of GaN based devices as claimed [3][4], essentially depend upon various factors. These include the quality of the epi – layer stack [5][6], along with the quality and the metal scheme implemented for the Ohmic and Schottky contacts [7][8]. The epi – layer engineering is focused towards minimizing grain boundaries and epitaxial defects for boosting the RF performance [6][9]. On the other hand, Ohmic metal engineering is specifically focused towards the reduction of contact resistance for compatibility towards high – speed operation [7][10], as opposed to the Schottky contact engineering which has a specific target towards achieving a lower gate leakage current all the while ensuring good adhesion towards the underlying epi – layer stack [8][11]. Commonly used metals include Ti [12], Pt [13], Ni [12], as possible candidates among the traditional metal stacks to improve the Schottky parameters such as the barrier height (Φ), ideality factor (η), thermal stability, and gate leakage current in an effort to improve the device reliability for mm – Wave applications. A Pt - based contact, for instance, as reported exhibits a higher Schottky barrier height [14][15] compared to the standard choice employing Ni - based contacts [16-18], and in essence would benefit power devices for mm – Wave operation specifically with short gate lengths as a courtesy of reducing the gate leakage current. As such, the demand for high frequency applications propels aggressive scaling of the GaN HEMTs in an attempt to target high frequency applications. This, however, is coupled with short channel effects (SCEs) due to which, a shorter gate loses its control over the 2D electron gas (2DEG)

channel. In this regard, to ascertain long - term reliability of GaN based devices, good quality Schottky contacts are required, which is the basis of this work.

This manuscript focuses on the reliability of Gate contacts for mm – Wave GaN HEMT devices sporting a gate length (L_G) of 150 nm. In this regard, two Schottky metal schemes based on Ni/Au and Pt/Au are considered, and the Gate contacts of the fabricated devices are subjected to a high field reverse bias step stress in an attempt to deliberately push the devices towards high gate leakage region. The manuscript is structured as follows. Section 2 gives a brief description about the fabrication aspects of the GaN HEMT devices considered in this work, while the reliability-based studies considering the two metal schemes are compiled in Section 3. Finally, the findings of this study are summarized in Section 4.

2. Experimental Methodology: The epi-layer structure of the Metal – Organic Chemical Vapor Deposition (MOCVD) based AlGaN/GaN HEMTs fabricated in this work is shown in Fig. 1(a). Starting from the SiC substrate, a 100 nm AlN nucleation layer is grown to reduce the lattice mismatch. Post the AlN growth, a 2.2 µm thick GaN buffer is grown which supports a 22 nm AlGaN barrier with an Aluminium concentration of 25%. The SEM micrograph depicting the Gate, Source, and Drain pad is shown in Fig. 1(b). Characterizing the epi – layer stack through hall measurements, reveal a 2DEG concentration of 1.1×10^{13} cm^{-2} and a carrier mobility of 1910 $cm^2V^{-1}s^{-1}$. The experimental processing steps are detailed in author's previous works [7][8]. A standard Ohmic metal scheme based on Ti, Al, Ni and Au is employed which is treated in rapid thermal annealing (RTA) in N_2 Ambient at 820 °C for 60 sec, for subsequent alloying. Passivation of the device is done by SiN_x using the plasma-enhanced chemical vapour deposition technique (PECVD) and gate slit opening. This is followed up by the Gate metal deposition with metal schemes Ni/Au (left - half) and Pt/Au (right - half) of 3" wafer (as shown in Fig. 2) with gate length, L_G = 150 nm, using the e-beam evaporation technique [19].

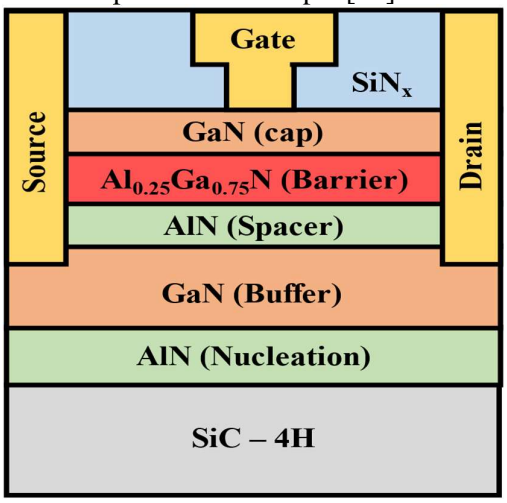

(a)

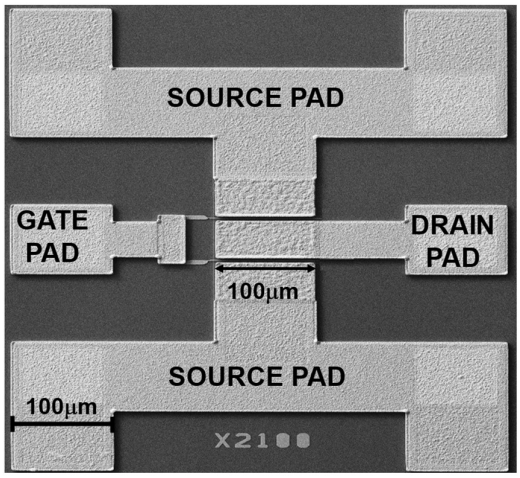

(b)

Figure 1. (a) Schematic representation, and (b) SEM Micrograph of the fabricated device having a Gate Length of 150 nm.

The source-drain terminals are 4 µm apart with a central gate placement. The DC – IV characterization of the fabricated devices was carried out using Keysight's Parametric Analyzer B1500A, revealing a high current density (I_{DS}) of 1.05 A/mm and a transconductance (g_m) of 250 mS/mm. The threshold voltage (V_{TH}) of the device as extracted from the transfer characteristics is – 5.8 V, and the ON – Resistance as extracted from the output characteristics is 3.3 Ω.mm.

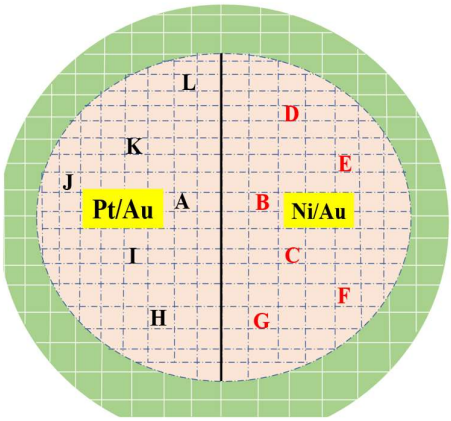

Figure 2. Schematic representation of 3-inch wafer with both (Pt/Au and Ni/Au) metal schemes.

To check the uniformity of the fabricated devices, six devices were characterized on each side of the wafer as shown in Fig. 2. The resulting DC characteristics of these devices are summarized in Table 1. It is observed that the maximum drain current (I_{DS}), peak transconductance (g_m), and the pinch – off voltage (V_{TH}) measured across 6 locations on each side of the wafer have a lower degree of deviation from their mean values, indicating a higher degree of uniformity throughout the wafer.

Table 1. List of parameters of measured devices at different positions with both the metal schemes

Location	Parameters		
	I_{DS} (A/mm)	g_m (mS/mm)	V_{TH} (V)
A	1.050	250	-5.80
I	1.045	248	-5.82
H	1.040	245	-5.82
J	1.044	248	-5.85
K	1.048	246	-5.80
L	1.042	244	-5.83
B	1.035	245	-5.80
C	1.032	243	-5.85
D	1.031	240	-5.80
E	1.028	241	-5.95
F	1.035	242	-5.80
G	1.030	238	-5.82

3. Results & Discussions

This section compares the Ni/Au and Pt/Au Schottky metal schemes in terms of two and three terminal characteristics followed by the reliability assessment as a means of validating and testing the fabricated AlGaN/GaN HEMT devices for mm-Wave applications.

3.1. Two terminal diode measurements

Forward and reverse characteristics of the Schottky diode of metal Ni/Au and Pt/Au are shown in Fig. 3. The Schottky parameters (Φ_B and η) of the two metal schemes were extracted (compiled in Table 2) using the thermionic emission (TE) [20] model at room temperature (T = 27 °C) by employing the standard diode Equation (1) and Equation (2):

$$I = I_S \left[\exp\left(\frac{qV - IR_D}{\eta kT}\right) - 1\right] \quad (1)$$

$$I_S = AA^*T^2 \exp\left(-q\,\Phi_B / kT\right) \quad (2)$$

Where, q : carrier charge,
k : Boltzmann's constant,
T : Temperature,
Φ_B : Schottky barrier height,
η : ideality factor,
A : diode area,
IR_D : voltage drop across the diode,
I_S : reverse saturation current, and
A* : Richardson constant for AlGaN

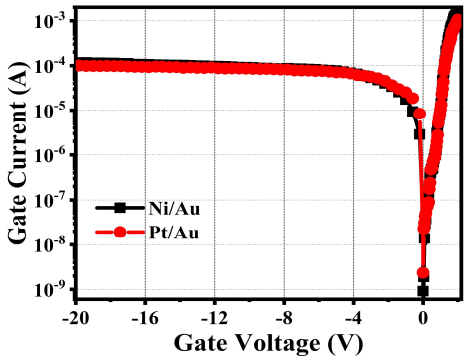

Figure 3. Two terminals forward and reverse characteristics for Ni/Au and Pt/Au Schottky metal schemes.

Table 2. Comparison of Schottky Parameters for the two metal schemes.

Schottky Metal	Parameters	
	ϕ_B (eV)	η
Ni/Au	0.562	1.28
Pt/Au	0.635	1.25

As shown in Table 2, Pt/Au metal has a higher barrier height and lower ideality factor compared to Ni/Au. This is due to the high work function of Pt metal [21, 22]. From Fig. 3, Pt/Au metal scheme has a lower leakage current compared to Ni/Au. This is due to metal-semiconductor surface inhomogeneities

and the higher metal work function of Pt metal [23-25].

3.2. Three terminal device measurements

Output Characteristics of L_G = 150 nm, W_G = 6 × 100 µm AlGaN GaN HEMT are shown Fig. 4 (a) and (b). The maximum drain current is 1.050 A/mm and 1.035 A/mm and transconductance is 250 mS/mm and, 245 mS/mm with Pt/Au and Ni/Au metal schemes, respectively.

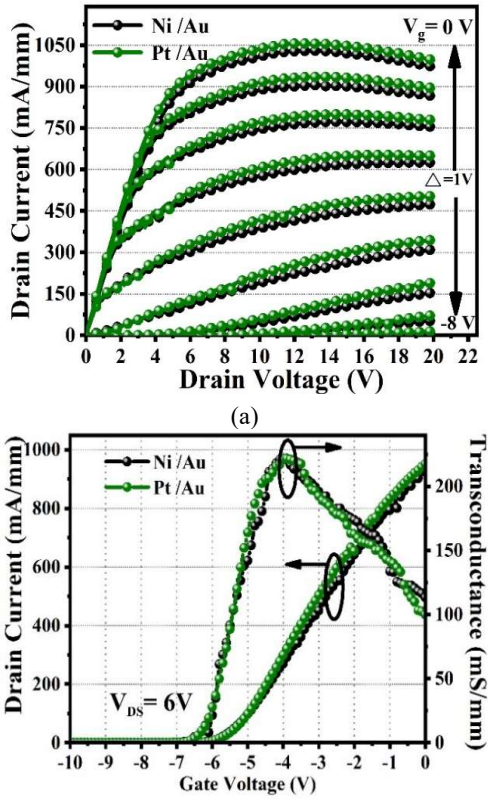

Figure 4. Impact of Ni/Au and Pt/Au Schottky metal schemes on (a) Output, and (b) Transfer characteristics of AlGaN/GaN HEMTs.

When the gate length is small in comparison to the barrier layer, aspect ratio ($L_G/t_{Barrier}$) ≤ 15, Short channel effects play a very important role [26, 27]. Here, with L_G = 150 nm and a barrier with 25 nm, the aspect ratio is 6. At higher drain to source voltage, V_{DS} (>10V), the confinement of the charge carrier becomes poor [27]. As shown in Fig. 5, with the increase in V_{DS}, a strong V_{TH} shift is observed. To pinch off the channel, the gate depletion region needs to be extended which results in a shift in V_{TH}. In shorter gate length devices, as V_{DS} increases, a high electric field drifts the charge carriers and the gate loses the control of flow of charge carriers and this phenomenon is known as drain-induced barrier lowering (DIBL) [24-27].

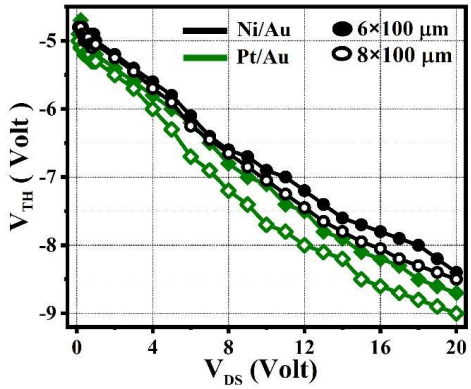

Figure 5. Spread of V_{TH} extracted at 1 mA/mm as a function of drain bias (V_{DS}) for the two Schottky metal schemes for large periphery GaN HEMT devices.

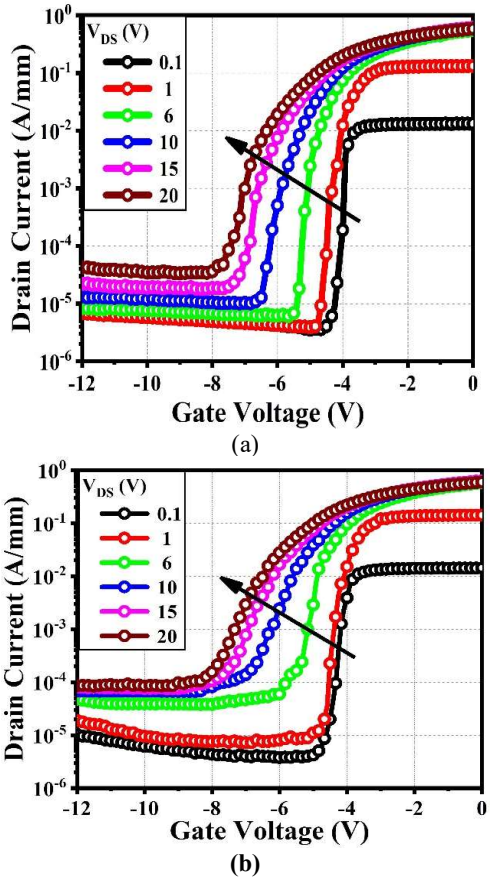

Figure 6. Transfer characteristics of 6×100 µm AlGaN/GaN HEMT at different V_{DS} (0.1, 1, 6, 10, 15 and 20 V) with L_G=150nm (V_{GS} swept from -12 to 0

V), for (a) Ni/Au, and (b) Pt/Au Schottky Gate contacts.

Figures 6 (a) and (b) show that Pt/Au has a higher V_{TH} compared to Ni/Au. This may be due to Metal - Semiconductor interface inhomogeneities [21, 22]. This shows that, in high voltage applications, the device with Pt/Au-based Schottky contact, shows a degradation in the device performance against the Ni/Au-based contact.

3.3. RF characterization

The device current gain($|H_{21}|$) of both the metal schemes is shown in Fig. 7. The device with Ni/Au and Pt/Au metal schemes has cutoff frequencies (F_T) of 38 GHz and 36 GHz, respectively. The maximum unilateral gain (MUG) indicates the maximum oscillating frequency (F_{MAX}) of the device, which is 60 GHz for the Ni/Au and 54 GHz for the Pt/Au scheme. Accordingly, the Ni/Au based metal scheme points towards achieving a better RF performance owing to its lower gate resistance compared to the Pt/Au metal scheme.

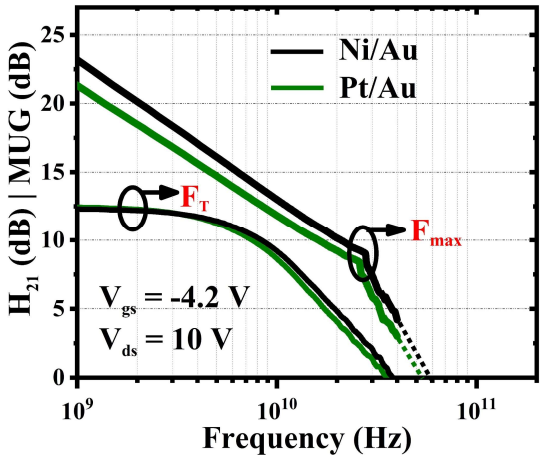

Figure 7. RF characteristics of the devices with Ni/Au and Pt/Au metal schemes.

3.4. Reverse bias step stress measurement

In the step stress measurement method, stress is applied to the gate terminal over some time, and gate current is observed. In this experiment, the V_{GS} is stepped up by -5V, and the gate current is observed for 120 seconds. The results of high reverse bias gate voltage step stress are shown in Fig. 8 (a) and (b). The findings suggest that leakage remains recoverable up to a gate voltage of -20V, attributed to the trapping of electrons beneath the gate region. Above -20V, the gate current becomes noisy and undergoes a significant increase, signaling degradation in device performance in both the metal scheme Ni/Au and Pt/Au as shown in Fig. 8(a). Gate voltage exceeding 25V (absolute value) shows irreversible degradation.

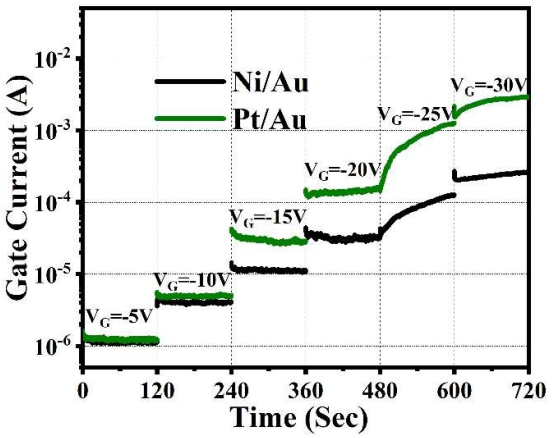

(a)

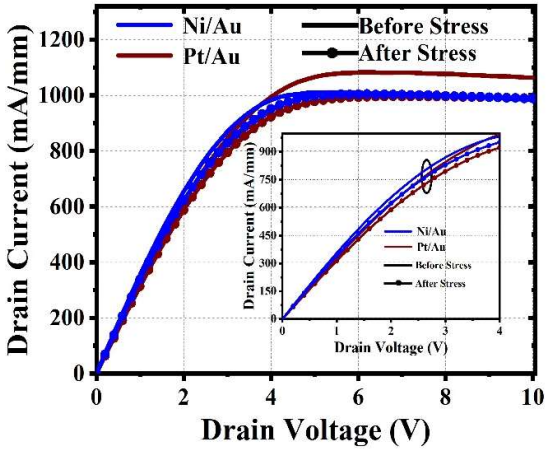

(b)

Figure 8. Reverse bias step stress scheme depicting (a) evolution of Gate current as a function of transient time, and (b) impact on R_{ON} calculated post high field stress.

As high voltage is applied to the gate terminal, the vertical electric field in the device increases which induces paths for current and rise in the gate current is observed [30-33]. Also, a high electric field deteriorates the crystallography of the barrier layer and induces an inverse piezoelectric phenomenon. However, due to M-S interface inhomogeneities, Pt/Au shows a higher leakage current rise compared to Ni/Au.

Also, Zanoni *et al*. [32] reported through electroluminescence (EL) analysis that hot spot formation at the gate edge under high reverse bias contributes to the rise in leakage current. DC characterization is carried out before and after each step of stress. To observe the current collapse phenomenon, or more appropriately an increase in the On-resistance (R_{ON}) of the device. Fig. 8(b) shows the increase in the R_{ON} after stress in both cases. Table 3, summarizes the change in the parameter after stress.

Table 3. Change in device parameters before and post high field electrical stress.

Parameters		Metal Scheme	
		Ni/Au	Pt/Au
I_{DS} (mA/mm)	Before Stress	1000	1060
	After Stress	980	980
	Change (%)	2	8
R_{ON} (Ω·mm)	Before Stress	3.65	3.62
	After Stress	4.50	5.0
	Change (%)	23.28	38.12

A significant change (in %) with Pt/Au-based contact is observed compared to Ni/Au post-high voltage reverse bias step stress. Chakraborty *et al*. [34] have also reported that Pt/Au-based Schottky gate contact tends to degrade with temperature and electrical stress compared to Ni/Au-based contacts.

4. Conclusions

Ni/Au and Pt/Au-based Schottky Gate contacts were realized on epi–layer stack consisting of AlGaN/GaN HEMTs for targeting mm–Wave applications. While the initial comparison based on Schottky parameters points towards Pt/Au to be the preferred choice for Gate contacts due to comparatively higher barrier height and lower gate leakage current, the Ni/Au-based contacts as investigated exhibit better reliability when subjected to a high field stress. A reverse bias strep stress subjected to two metal schemes reveals a degradation of 8% and ~38% in I_{DSS} and R_{ON}, respectively in the case of Pt/Au contacts against the 2% and ~24% degradation recorded in Ni/Au contacts for the I_{DSS} and R_{ON}, respectively. In addition to these, due to the improvement in barrier inhomogeneities with the Ni/Au-based contact, the GaN HEMT with Ni-based contacts demonstrate a smaller spread in V_{TH} with applied drain bias, pointing towards a better suppression of the SCEs compared to the Pt-based contacts. These results point towards the remarkable performance of Ni/Au-based Schottky metal contacts for Ku–band applications.

Acknowledgement

The authors would like to acknowledge Dr. Meena Mishra (Director) of SSPL, DRDO for providing the facilities and necessary support. The authors are thankful to the GaN fabrication group of SSPL for technical support and discussion.

CRedit Author Statement

Chanchal: Conceptualization, Methodology, Visualization, Data analysis and interpretation, Investigation and Writing – Original Draft.
Khushwant Sehra: Methodology, Writing-Reviewing and Editing, Proofreading.
Amit Malik: Visualization, Supervision, Technical Inputs.
Robert Laishram: Technical Inputs and Proofreading.
Dipendra Singh Rawal: Supervision, Writing- Reviewing and Editing, Validation, Technical Inputs and Resources.
Manoj Saxena: Supervision, Proofreading, Writing- Reviewing and Editing, Technical Inputs.

Conflict of Interest

Authors declare No conflicts of interest.

References

[1] S. Krause *et al.,* "AlScN/GaN HEMTs Grown by Metal-Organic Chemical Vapor Deposition With 8.4 W/mm Output Power and 48 % Power-Added Efficiency at 30 GHz," in IEEE Electron Device Letters, vol. 44, no. 1, pp. 17-20, Jan. 2023, doi: 10.1109/LED.2022.3220877.

[2] N. Collaert *et al.,* "III-V/III-N technologies for next generation high - capacity wireless communication," in International Electron Devices Meeting (IEDM), pp. 11.5.1-11.5.4, Dec. 2022, doi: 10.1109/IEDM45625 .2022.10019555.

[3] P. Wang *et al.,* "Evaluation of Power and Linearity at 30 GHz in AlGaN/GaN HEMT Fabricated by Integrating Transistors With Multiple Threshold Voltages," in IEEE Transactions on Electron

Devices, vol. 71, no. 3, pp. 1421-1427, March 2024, doi: 10.1109/TED.2023.3347710.

[4] A. Hickman *et al.*, "2.2 W/mm at 94 GHz in AlN/GaN/AlN High Electron Mobility Transistors on SiC," in Physica Status Solidi A, vol. 220, no. 16, January 2023, doi: 10.1002/pssa.202200774.

[5] A. S. Razeen *et al.*, "Structural, optical, and electrical characterization and performance comparison of AlGaN/GaN HEMT structures with different buffer layers," in Vacuum, vol. 219, art. no. 112704, January 2024, doi: 10.1016/j.vacuum.2023.112704.

[6] D.-Y. Chen *et al.*, "Impact of the Channel Thickness on Electron Confinement in MOCVD-Grown High Breakdown Buffer-Free AlGaN/GaN Heterostructures," in Physica Status Solidi A, vol. 220, no. 16, art. no. 2200496, September 2022, doi: 10.1002/pssa.202200496.

[7] A. K. Visvkarma *et al.*, "Ohmic contact morphology improvement with reduced resistance using Si/Au/Ti/Al/Ni/Au (AlGaN) and Si/Au/Ti/Al/Ni/Au (InAlN) stack layers in III-Nitride HEMTs," in Semiconductor Science and Technology, vol. 37, no. 8, art. no. 085006, June 2022, doi: 10.1088/1361-6641/ac6f79.

[8] A. K. Visvkarma *et al.*, "Comparative study of Au and Ni/Au gated AlGaN/GaN high electron mobility transistors," in AIP Advances, vol. 9, no. 12, art. no. 12531, December 2019, doi: 10.1063/1.5116356.

[9] D. M. Fleetwood *et al.,* "Low-Frequency Noise Due to Iron Impurity Centers in GaN-Based HEMTs," in IEEE Transactions on Electron Devices, vol. 71, no. 2, pp. 1024-1030, Feb. 2024, doi: 10.1109/TED.2023.3347212.

[10] Z. Xie *et al.,* "Ta/Al/CuW low temperature ohmic contacts for GaN-on-Si HEMT," in Microelectronic Engineering, vol. 286, art. no. 112132, March 2024, doi: 10.1016/j.mee.2024.112132.

[11] X. Ding *et al.*, "Gate leakage mechanisms of the AlGaN/GaN HEMT with fluorinated graphene passivation," in Materials Science in Semiconductor Processing, vol. 162, art. no. 107502, August 2023, doi: 10.1016/j.mssp.2023.107502.

[12] A. E. Islam *et al.*, "Effect of High Temperature on the Performance of AlGaN/GaN T-Gate High-Electron Mobility Transistors With ~140-nm Gate Length," in IEEE Transactions on Electron Devices, vol. 71, no. 3, pp. 1805-1811, March 2024, doi: 10.1109/TED.2024.3353694.

[13] S. Alam *et al.,* "Estimation of electrostatic, analogue, Linearity/RF figures-of-merit for GaN/SiC HEMT," in Micro and Nanostructures, vol. 186, art. no. 207738, February 2024, doi: 10.1016/j.micrna.2023.207738.

[14] E. Akso *et al.*, "Schottky Barrier Gate N-Polar GaN-on-Sapphire Deep Recess HEMT With Record 10.5 dB Linear Gain and 50.2% PAE at 94 GHz," in IEEE Microwave and Wireless Technology Letters, vol. 34, no. 2, pp. 183-186, Feb. 2024, doi: 10.1109/LMWT.2023.3345531.

[15] N. Miura *et al.*, "Effects of interfacial thin metal layer for high-performance Pt-Au-based Schottky contacts to AlGaN-GaN," in IEEE Transactions on Electron Devices, vol. 51, no. 3, pp. 297-303, March 2004, doi: 10.1109/TED.2003.822472.

[16] L. Liu *et al*., "Comparison of DC performance of Pt/Ti/Au- and Ni/Au-gated AlGaN/GaN high electron mobility transistors," in Journal of Vacuum Science & Technology B, vol. B29, art. no. 042202, July 2011, doi: 10.1116/1.3607601.

[17] S. Bouzid-Driad *et al.*, "Optimization of AlGaN/GaN HEMT Schottky contact for microwave applications," in European Microwave Integrated Circuit Conference, pp. 119-122, 2012.

[18] K. Floros *et al.,* "Dual barrier InAlN/AlGaN/GaN-on-silicon high-electron-mobility transistors with Pt- and Ni-based gate stacks: Dual barrier InAlN/AlGaN/GaN-on-silicon high-electron-mobility transistors" in Physica Status Solidi (A) Applications and Materials, vol. 214, no. 8, art. no. 1600835, July 2017, doi: 10.1002/pssa.201600835.

[19] Chanchal *et al*., "Physical insights into the reliability of sunken source connected field plate GaN HEMTs for mm-wave applications", in Microelectronics Reliability, vol. 148, art. no. 115170, 2023, doi: 10.1016/j.microrel.2023.115170.

[20] Wu Mei *et al.,* "Schottky forward current transport mechanisms in AlGaN/GaN HEMTs over a wide temperature range", in Chinese Phys. B, vol. 23, no. 9, art. no. 097307, 2014, doi: 10.1088/1674-1056/23/9/097307.

[21] Sun *et al.,* "Review of the recent progress on GaN-based vertical power Schottky barrier diodes (SBDs)," in Electronics, vol. 8, no. 5, pp. 1 – 15, 2019, doi: 10.3390/electronics8050575.

[22] B. Ofuonye *et al.,* "Electrical and microstructural properties of thermally annealed Ni/Au and Ni/Pt/Au Schottky contacts on AlGaN/GaN heterostructures," in Semiconductor Science and Technology, vol. 29, no. 9, pp. 1 – 10, 2014, doi: 10.1088/0268-1242/29/9/095005.

[23] A. K. Visvkarma *et al.*, "Improvement in Schottky barrier inhomogeneities of Ni/AlGaN/GaN Schottky diodes after cumulative γ-ray irradiation", in Semiconductor Science and Technology, vol. 36, no. 6, art. no. 065012, pp. 1 – 10, 2021, doi: 10.1088/1361-6641/abf46d.

[24] M. A. Laurent *et al.*, "Barrier height inhomogeneity and its impact on (Al,In,Ga)N Schottky diodes", in Journal of Applied Physics, vol. 119, no. 6, art. no. 064501, pp. 1 – 7, 2016, doi: 10.1063/1.4941531.

[25] S. Karboyan, *et al.,* "Analysis of barrier inhomogeneities in AlGaN/GaN HEMTs' Schottky diodes by I-V-T measurements," in European

Microwave Integrated Circuit Conference, Nuremberg, Germany, pp. 240-243, 2013.

[26] O. Breitschädel *et al.*, "Short-channel effects in AlGAN/GaN HEMTs," in Materials Science and Engineering B-advanced Functional Solid-state Materials, vol. 82, no. 1 – 3, pp. 238 - 240, 2001, doi: 10.1016/S0921-5107 (00)00747-9.

[27] M. Nuo *et al*., "Gate/Drain Coupled Barrier Lowering Effect and Negative Threshold Voltage Shift in Schottky-Type p-GaN Gate HEMT," in IEEE Transactions on Electron Devices, vol. 69, no. 7, pp. 3630 - 3635, July 2022. doi:10.1109/ TED.2022.3175792.

[28] Charu *et al.,* "Suppression of Short-channel Effects by Double-gate Double-channel Device Design in Normally-off AlGaN/GaN MIS-HEMTs," in IETE Journal of Research, vol. 67, no. 3, pp. 425 – 432, 2021, doi: 10.1080/03772063.2018. 1541764.

[29] K. Harrouche *et al*., "Low Trapping Effects and High Electron Confinement in Short AlN/GaN-on-SiC HEMTs by Means of a Thin AlGaN Back Barrier," in Micromachines, vol. 14, no. 2, pp. 1 - 7, 2023, doi: 10.3390/mi14020291.

[30] Meneghesso *et al.,* "Degradation of AlGaN/GaN HEMT devices: Role of reverse-bias and hot electron stress," in Microelectronic engineering, vol. 109, pp. 257-261, 2013, doi: 10.1016/j.mee. 2013.03.017.

[31] Meneghesso *et al.,* "Reliability of GaN high-electron-mobility transistors: State of the art and perspectives," in IEEE Transactions on Device and Materials Reliability, vol. 8, no. 2, pp. 332 – 343, 2008, doi: 10.1109/TDMR.2008.923743.

[32] E. Zanoni *et al.,* "Localized damage in AlGaN/GaN HEMTs induced by reverse-bias testing," in IEEE Electron Device Letters, vol. 30, no. 5, pp. 427 – 429, 2009, doi:10.1109/LED.2009. 2016440.

[33] J. A. del Alamo *et al.*, "GaN HEMT reliability," in Microelectronics Reliability, vol. 49, no. 9 – 11, pp. 1200 – 1206, 2009, doi:10.1016/j.microrel. 2009.07.003.

[34] S Chakraborty *et al.,* "Comprehensive Schottky Barrier Height Behavior and Reliability Instability with Ni/Au and Pt/Ti/Pt/Au on AlGaN/GaN High-Electron Mobility Transistors," in Micromachines, vol. 13, no. 1, pp. 1 – 10, 2022, doi:10.3390/ mi13010084.